Coupled-channel calculation of stopping powers for intermediate-energy light ions penetrating atomic H and He targets

G. Schiwietz
Hahn-Meitner-Institut Berlin G.m.b.H., Department P3, Glienickerstrasse 100, D-1000 Berlin 39, Federal Republic of Germany
(Received 31 January 1990)

A single-center coupled-channel code based on an expansion in terms of atomic wave functions that includes dynamic curved projectile trajectories is applied to the calculation of stopping powers. Stopping powers and differential ionization cross sections are evaluated for $\bar{p}$, H^+, He^{2+}, and Li^{3+} projectiles penetrating atomic H and He targets at energies of 10–500 keV/u. The results are compared to experimental data, to predictions of the first-order plane-wave Born approximation, and to results of calculation for excitation of a harmonic oscillator including Barkas corrections. The improvement of the present model to first-order or second-order perturbative treatments as well as the effect of polarization on the projectile trajectories is discussed.

I. INTRODUCTION

The interaction of ions with dense matter has been investigated for decades.[1–5] Classical[1,2] as well as quantum-mechanical[3] theories have been applied to the calculation of electronic stopping powers. At low-energy ion-atom collisions the stopping power is dominated by electron capture and electron loss of projectile electrons.[2] At high incident energies excitation and ionization of target electrons are the most important energy-transfer mechanisms.[3] This was confirmed in numerous comparisons between experimental and theoretical stopping-power values.[6] However, it was shown recently[7] that exact classical three-body calculations are unable to predict cross sections for low-velocity ion-atom collisions where quasimolecular[8] effects come into play. For high incident energies[7] and low-momentum transfers[9] classical collision theories tend to underestimate the dipole contribution of excitation and ionization cross sections. Thus there is a need for quantum-mechanical collision theories with a large range of validity. The aim of this work is to describe an improved quantal collision theory applicable to the calculation of stopping powers for intermediate (about 50 keV/u) and high incident energies.

Quantal[3] and classical[9] models based on first-order perturbation theory predict all cross sections to be strictly proportional to Z_p^2, the squared projectile charge. However, Barkas and co-workers[10] found a difference between the ranges of π^+ and π^- particles, an indication for a contribution proportional to Z_p^3. Subsequent measurements of H and He stopping powers by Andersen, Simonsen, and Sørensen[11] confirmed the deviations from the Z_p^2 law. It is noted that positively charged particles may carry bound electrons during their passage through dense matter. In this case the projectile is screened, which leads to a reduced stopping power, or the projectile electrons contribute actively to the collision process, corresponding to an enhanced stopping power. Recently, a sign-of-charge dependence was found also in single-collision experiments for double ionization of He atoms by protons and antiprotons.[12] This effect was attributed to the "dynamic electron-electron correlation" influenced by the projectile Coulomb potential.[13]

In this work an approximate description of the electron-electron interaction is introduced in order to allow for comparison with experiments. The main attention will be given to higher-order effects in the case of bare incident ions. Such a higher-order effects are the increased binding,[14] electron capture (in case of a target-centered expansion), or multistep processes, generally denoted polarization effects. A standard expression for the lowest-order polarization effect, the so-called Barkas effect, was given by Ashley, Ritchie and Brandt.[15] However, since the Barkas term found by these authors actually diverges at small impact parameters a cutoff impact parameter had to be introduced.[15,16] Hill and Merzbacher[17] worked out a second-order quantal theory of stopping powers with the restriction to monopole and quadrupole transitions. It was pointed out that there is no physical reason to exclude the regime of small impact parameters except for asymptotically high velocities.[17] In fact, it was found experimentally that the influence of polarization effects at intermediate incident energies is even more pronounced at small impact parameters.[18,19]

Recently, Mikkelsen and Sigmund[20] performed second-order calculations similar to those of Hill and Merzbacher, but convergence with respect to the multipole expansion was achieved.[20] Mikkelsen and Sigmund give stopping-power values as well as Barkas corrections for targets described by a set of harmonic oscillators. The present work introduces an improved stopping-power theory where exact *atomic* target-centered wave functions, *damped continuum* wave packets, and *dynamic curved* projectile trajectories are incorporated. The calculations are carried out in highest order, so that the Barkas term is only one of the polarization effects taken into

account.

General model assumptions are outlined in Sec. II. In Sec. II A the numerical methods and the underlying approximations are explained and the calculation of stopping powers from transition probabilities is described in Sec. II B. Results of the present theory are presented and discussed in Sec. III. Unless indicated otherwise, atomic units (a.u.) are used throughout the paper ($e=\hbar=m_e=1$).

II. THEORY

The theoretical formulation of atomic excitation and ionization processes is conveniently discussed by introducing the quantum-mechanical Hamilton operator. For a three-body system the Hamiltonian reads

$$\mathcal{H}=T_p(\mathbf{r}_p)+T_t(\mathbf{r}_t)+T_e(\mathbf{r}_e)+V_{pt}(\mathbf{R})+V_{te}(\mathbf{r})+V_{pe}(\mathbf{R}-\mathbf{r}) , \tag{1}$$

with the kinetic and potential energies denoted T and V, respectively. The subscripts p, t, and e refer to the projectile ion, target core, and electron as indicated in Fig. 1.

In the following we will use the impact-parameter method, i.e., it is assumed that $\mathbf{r}_p$ and $\mathbf{r}_t$ are given by classical paths

$$\mathbf{r}_p=\mathbf{r}_p(t,b) \qquad \mathbf{r}_t=\mathbf{r}_t(t,b) . \tag{2}$$

This concept was first introduced by Bang and Hansteen.[21] It is well known[22] that the impact-parameter method is valid as long as the Coulomb parameter

$$\nu_{i\to f}=\frac{Z_pZ_tm_p}{q_{i\to f}}\approx\frac{Z_pZ_tv_pm_p}{\Delta E_{i\to f}} \tag{3}$$

is large compared to unity ($q_{i\to f}$ is the momentum transfer). This is always valid if the incident ion has at least thermal energies. If, additionally, an independent motion of the electrons[23] is assumed, one may solve the time-dependent Schrödinger equation for one active electron:

$$\left[i\frac{\partial}{\partial t}-\mathcal{H}_e(t)\right]\Phi_e(t)=0 , \tag{4}$$

with

$$\mathcal{H}_e(t)=\mathcal{H}_{te}+V_{pe}(\mathbf{R}(t)-\mathbf{r}) , \tag{4a}$$

$$V_{pe}(\mathbf{R}(t),\mathbf{r})=\frac{-Z_p}{|\mathbf{R}(t)-\mathbf{r}|} , \tag{4b}$$

$$\mathcal{H}_{te}=-V_t(\mathbf{r}_e-\mathbf{r}_t(t))+T_e(\mathbf{r}_e) . \tag{4c}$$

The operator V_t is taken to be a single-ζ Hartree-Fock potential as defined by Clementi and Roetti.[24] In the case of hydrogenlike targets V_t reduces to the pure Coulomb potential Z_t/r with target charge Z_t. The use of simple Hartree-Fock potentials excludes already initial and final-state electron correlation. Consequently, we adopt the independent-electron model, as described, e.g., by McGuire and Weaver,[23] and exclude also dynamic correlation effects during the collision as well as static Pauli correlation. It is noted that correlation effects and/or mean-field effects may become important for the excitation and ionization mechanisms if multielectron transitions come into play. This is the case for highly charged incident ions at low energies[25–27] or when the projectile carries electrons. Bound projectile electrons may screen the projectile nuclear charge as spectators or they may interact with target electrons resulting in enhanced excitation and ionization cross sections.[28]

In the subsequent treatment the electron coordinate will be measured from the accelerated target nucleus and is the only dynamical variable. Thus the target system is the frame of reference.[29,30] In such a noninertial system non-Newtonian forces arise. The corresponding Hamiltonian H_{te} is

$$\mathcal{H}_{te}=-V_t(\mathbf{r})+T_e(\mathbf{r})+V_{\text{recoil}}(\mathbf{r},\mathbf{r}_t(t)) . \tag{5}$$

It is reasonable to neglect the last term V_{recoil}. By doing this transitions are excluded which are due to the interaction of the active electron with the recoiling target nucleus. This so-called recoil effect leads to insignificant contributions to total cross sections, but may be important for very close collisions ($b<10^{-3}$ a.u.).[31]

Before the solution of Eq. (4) is explained in more detail, the classical path $\bar{R}(t)$ should be defined. Given the time-dependent electronic wave function Φ_e, a classical Hamiltonian for the heavy particles may be defined:

$$\mathcal{H}_h=T_p(\mathbf{r}_p)+T_t(\mathbf{r}_t)+V_{pt}(\mathbf{R})+\langle\Phi_e|V_{pe}(\mathbf{R}-\mathbf{r})|\Phi_e\rangle+\langle\Phi_e|V_{te}(\mathbf{r})|\Phi_e\rangle , \tag{6}$$

with

$$V_{pt}(\mathbf{R})=Z_pV_t(\mathbf{R}) . \tag{6'}$$

This equation is solved approximately by applying Newton's laws of motion as in the classical-trajectory Monte Carlo model.[32,33] The last term in Eq. (6) was neglected because of its small influence on the motion of

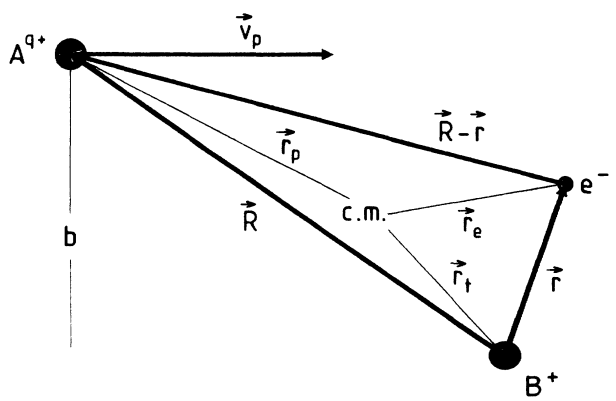

FIG. 1. Vector diagram for the bare ion (A^{q+}), the ionic target core (B^+), and one active electron (e^-). The impact parameter b is indicated. $\mathbf{r}_p$, $\mathbf{r}_t$, and $\mathbf{r}_e$ are position vectors of projectile, target, and electron in the center-of-mass system.

the target core in case of a strongly target-centered wave function Φ_e. It is emphasized that the concept defined by Eq. (6) introduces for the first time a dynamically curved projectile trajectory in the impact-parameter method. Thus the projectile motion is coupled to the motion of the active electron. However, since the projectile interacts with a mean electronic field, there is only approximate conservation of energy and momentum. For small projectile scattering angles this deficiency can be circumvented. In this case conservation of energy and momentum may be forced by applying the Eikonal transformation.[34]

It is noted that some calculations have been performed with hyperbolic projectile paths. In this case only the first three terms in Eq. (6) are considered. However, most of the previous calculations have been performed for straight line paths, as given by the first two terms in Eq. (6). Such calculations are equivalent to quantum-mechanical solutions of the three-body Schrödinger equation with plane projectile waves. Typical examples for such quantum-mechanical three-body theories are the plane-wave Born approximation[35] and its limiting form at high incident energies, the Bethe theory.[36] However, the main advantage of the present model compared to previous stopping-power theories is the highest-order (coupled-channel) description of the electronic motion. The corresponding calculation of excitation and ionization probabilities will be explained in Sec. II A.

A. Wave functions and collision dynamics

Generally, ion-atom collision processes may be described either by first- or second-order perturbative approaches or by coupled-channel calculations. Perturbation theory often yields simple and in some cases even analytical results, but has the disadvantage of being valid only for high incident energies and low projectile charge states. In this work we will use a highest-order (coupled-channel) theory which allows for an infinite number of interactions between projectile, target, and electron. The electron may be ionized in a first step and may be accelerated or decelerated in a second step. It is also possible that an electron, after being ionized, is "thrown" back to the initial state. Furthermore, the probability for ionizing an electron is always less than or equal to unity. All this does not hold for perturbation theory. In the following, the basic ingredients of our model will be described.

The starting point of the present theory is an expansion of the time-dependent electronic wave function Φ_e in terms of single-center eigenfunctions φ_i of the target Hamiltonian H_{te},

$$\Phi_e(\mathbf{r},t)=\Phi_B(\mathbf{r},t)+\Phi_C(\mathbf{r},t)\ , \tag{7}$$

$$\Phi_B(\mathbf{r},t)=\sum_{n,l,m} a_{n,l,m}(t)e^{-iE_{n,l}t}\varphi_{n,l,m}(\mathbf{r})\ , \tag{7a}$$

$$\Phi_C(\mathbf{r},t)=\sum_{l,m}\int_0^\infty d\varepsilon\, b_{l,m}(\varepsilon,t)e^{-i\varepsilon t}\varphi_{\varepsilon,l,m}(\mathbf{r})\ . \tag{7b}$$

The eigenfunctions φ_i are defined in the usual way as

$$\varphi_{n,l,m}(\mathbf{r})=\frac{1}{r}u_{n,l}(r)Y_{l,m}(\Theta,\phi) \tag{8}$$

and

$$E_{n,l}u_{n,l}(r)=\left[\frac{-d^2}{2dr^2}+\frac{l(l+1)}{2r^2}-V_t(r)\right]u_{n,l}(r)\ , \tag{9}$$

where $E_{n,1}$ and the subscript n have to be replaced by ε for continuum states.

For radial wave functions $u_{n,l}$ and $u_{\varepsilon,l}$ are calculated numerically using a Runge-Kutta method with variable step width. The bound-state wave functions $u_{n,l}$ are integrated from large r values down to zero and free wave functions are calculated from zero towards large r in order to suppress any irregular component in the wave function. The numerical uncertainty of the bound-state eigenvalues $E_{n,l}$ is about 10^{-6} eV. Boundary values for small r are obtained from a polynomial expansion of V_t and $u_{\varepsilon,l}$.[37] The normalization of continuum states is similar to the method described by Cowan.[38] Bound-state wave functions are dimensionless whereas the continuum states are normalized per square root of energy (in a.u.). Hence it follows from Eq. (7b) that the coefficients $b_{l,m}$ are also given per square root of energy (in a.u.). The eigenfunctions of H_{te} should be complete and orthogonal. The completeness was checked by calculating the overlap matrix elements between an arbitrary target-centered wave function and Φ_e. The sum over the corresponding squared overlap matrix elements was equal to unity to within 10^{-4} or better. Orthogonality was verified by calculating overlap matrix elements between different eigenfunctions φ_i which are typically in the order of 10^{-5}.

The infinite sums in Eqs. (7a) and (7b) have to be truncated in order to perform the numerical calculation of the time-dependent wave function or the corresponding coefficients a and b. This introduces no problems for the bound states since highly excited states are generally less populated than the K, L, or M shell. However, electrons captured into projectile states, as well as high-energy continuum electrons, lead to a population of high l states of target-centered wave functions. Thus partial waves up to orbital angular momenta of $l=8$ are considered for the continuum states. Another problem arises since the continuous energy variable of the free wave functions is not easy to handle in a numerical calculation. Therefore the continuum is represented by a sum over a few (about ten for each orbital angular momentum in the present work) pseudodiscrete radial wave functions $\Psi_{l,m}$:

$$\Phi_C(\mathbf{r},t)=\sum_{j,l,m}\frac{1}{r}\Psi_{l,m}(\varepsilon_j-\Delta\varepsilon j/2,\varepsilon_j+\Delta\varepsilon j/2,r,t)\times Y_{l,m}(\Theta,\phi)\ , \tag{10}$$

$$\Psi_{l,m}(E_1,E_2,r,t)=\int_{E_1}^{E_2}d\varepsilon\, b_{l,m}(\varepsilon,t)e^{-i\varepsilon t}u_{\varepsilon,l}(r)\ . \tag{10'}$$

An exact solution for $\Psi_{l,m}$ may be given in case of a pulselike ionization process at $t=0$. The corresponding moving wave packet is known as a Weyl packet,[39,40]

$$\Psi_{l,m}(E_1,E_2,r,t)\approx\bar{b}_{l,m}(\bar{\varepsilon},t)\int_{E_1}^{E_2}d\varepsilon\, e^{-i\varepsilon t}u_{\varepsilon,l}(r)\ . \tag{11}$$

However, the numerical treatment of such explicitly time-dependent basis states would be time consuming compared to the treatment of bound states. Thus we search for a further simplification of $\Psi_{l,m}$ by investigating the asymptotic behavior of Coulomb wave functions.[38] For $r\Delta\varepsilon \ll \pi$ the radial wave function $u_{\varepsilon,l}$ is nearly independent of ε and may be considered constant for the integration. For $\varepsilon t \ll \pi$ the exponential function in Eq. (11) is nearly independent of ε. In both cases $\Psi_{l,m}$ in Eq. (11) may be replaced by

$$\begin{aligned}\Psi_{l,m}(E_1,E_2,r,t)&\approx\frac{\bar{b}_{l,m}(\bar{\varepsilon},t)}{E_2-E_1}\left[\int_{E_1}^{E_2}d\varepsilon\, e^{-i\varepsilon(t-t_0)}\right]\left[\int_{E_1}^{E_2}d\varepsilon\, u_{\varepsilon,l}(r)\right]\\&=\bar{b}_{l,m}(\bar{\varepsilon},t)e^{-i\bar{\varepsilon}t}F(E_2-E_1,t)\int_{E_1}^{E_2}d\varepsilon\, u_{\varepsilon,l}(r)\\&=\frac{\bar{a}_{l,m}(\bar{\varepsilon},t)}{(E_2-E_1)^{1/2}}e^{-i\bar{\varepsilon}t}F(E_2-E_1,t)\int_{E_1}^{E_2}d\varepsilon\, u_{\varepsilon,l}(r)\ ,\end{aligned} \tag{12}$$

with

$$F(\Delta E,t)=\begin{cases}\dfrac{2}{t\Delta E}\sin\left[\dfrac{t\Delta E}{2}\right]\\ 1\quad\text{otherwise}\end{cases}$$

for continuum states and $t>0$ (12′)

The dimensionless coefficients $\bar{a}$ correspond to the coefficients $\bar{b}$ defined above. Except for $\bar{a}$ and the exponential function in Eq. (12), all quantities are real numbers and only the integral over the radial continuum wave functions needs to be calculated numerically. A damping function similar to F was introduced by Reading *et al.*[41] in order to improve the asymptotic behavior of continuum wave functions. However, the wave packets as described above are only approximate solutions for large values of t and r. It is evident that this deficiency will affect mainly those continuum states which have a considerable overlap with asymptotic projectile states. Most of these states are neglected anyway because of the finite number of target-centered partial waves ($l<9$) taken into account.

From the structure of Coulomb wave functions it is obvious that transition matrix elements involving either a high Rydberg state or a low-energy continuum state are identical when normalized per square root of energy.[38] Thus approximate completeness of the basis set may be achieved, although an infinite number of high-lying Rydberg states is not explicitely considered in Φ_e. This is done by renormalizing the energy width (E_1-E_0) of the lowest-energy continuum states so that the corresponding wave packets include a contribution of high Rydberg states.

In the present work the time-dependent Schrödinger equation is solved without any further approximations. Thus probabilities and cross sections computed with this method should be highly accurate as long as electron capture by the projectile is of minor importance. This corresponds to incident energies down to the maximum of the stopping-power curve (>50 keV). However, reasonable convergence was achieved down to about 10 keV/u by choosing appropriate basis sets to simulate the electron capture. It is noted that other authors have either neglected the damping factor F,[39,40] or they used only approximate atomic wave functions[41] in similar descriptions of the electronic motion.

It is obvious that the representation of Φ_C may be improved for large t by using the time-dependent Weyl packets [Eq. (11)] for $\Psi_{l,m}$. However, especially for high projectile charges ($Z_p/v_p \gg 0.3$) two-center effects may strongly influence the ionization mechanism.[42,43] In this case two-center wave functions are appropriate to describe the continuum,[44] but at present it is not clear how to construct reasonable two-center wave packets for coupled-channel theories. A two-center description of Φ_e is also necessary if electron capture into asymptotically bound projectile states is considered. In this case projectile-centered traveling orbitals have to be included in the expansion of Φ_C [Eq. (7b)].[45] The approximate dynamical treatment of only one additional projectile-centered state drastically improves the description of the time-dependent wave function.[46] Full two-center[47,48] or even triple-center[49] theories may be applied in principle to all collision systems independent of projectile charge or velocity. However, the corresponding computation of cross sections is time consuming, and until now only approximate atomic continuum states were included in these models.

The solution of the only unknown variables, namely the coefficients $a_{n,l,m}$, is straightforward. The definition of Φ_e [Eqs. (7), (10), and (12)] for small t is inserted into the time-dependent Schrödinger equation. The resulting equation is multiplied with an arbitrary eigenfunction φ_f^* and integrated over the $\mathbf{r}$ coordinate. Furthermore, orthogonality and the eigenvalue equation [Eq. (9)] are considered. Consequently, an infinite system of coupled first-order differential equations (coupled-channel equations) defines the time evolution of $a_{n,l,m}$,

$$\frac{d}{dt}a_{j',l',m'}(t)=\sum_{j,l,m}a_{j,l,m}(t)e^{i(E_{j',l'}-E_{j,l})t}\times V_{pe}^{j,l,m\to j',l',m'}(\mathbf{R}(t))\ , \tag{13}$$

with

$$\mathcal{V}_{pe}^{i\to f}(\mathbf{R}(t))=\langle\varphi_f|V_{pe}(\mathbf{R}(t),\mathbf{r})|\varphi_i\rangle \tag{13'}$$

and

$$\lim_{t\to-\infty} a_{n,l,m}(t)=\delta_{1s_0,nl_m}$$

for H and He ground state targets.

The interaction potential V_{pe} is replaced by its multipole expansion.[31,45] Thus the Coulomb matrix elements $\mathcal{V}_{pe}^{i\to f}$ are reduced to finite sums over weighted radial integrals, the so-called form factors. The form factors are computed numerically for all nonzero multipole terms. The weight factors are determined by Wigner $3j$ symbols. For transitions from a continuum state to any state the damping factor F [Eq. (12')] was included. For those transition matrix elements where the final state is a continuum wave packet the corresponding damping factor was set unity. This improves the coupled-channel results for small projectile charges. On the other hand, the coefficients $a_{j,l,m}$ have to be unitarized after each integration step. It is noted that this unitarization affects the transition probabilities by about 5% in the worst case considered for incident protons (10-keV H^++H,He).

From symmetry properties of the wave function and from the Coulomb matrix elements it is possible to distinguish between two classes of basis states, namely gerade and ungerade states. The corresponding wave functions Φ^+ and Φ^- may be obtained by replacing the spherical harmonics $Y_{l,m}$ in Eq. (8) by (see, e.g., Ref. 25)

$$Y_{l,|m|}^{\pm}=\frac{1}{\sqrt{2}}[Y_{l,|m|}\pm(-1)^m Y_{l,|m|}] \quad \text{for } m\neq 0 \tag{14a}$$

$$Y_{l,0}^{+}=Y_{l,0}\ . \tag{14b}$$

The Coulomb interaction does not lead to transitions between gerade and ungerade states. In this paper the initial state will be always $1s$, which is gerade. Thus the coupled-channel equations are solved in the present work for about 90 gerade states (10 bound states and 80 continuum states), which replace about 150 eigenstates. These gerade states are chosen to yield optimum convergence for a certain regime of incident energies. The corresponding excitation and ionization probabilities are given by projection on asymptotic target-centered states,

$$P_{n,l,m}(b)=\lim_{t\to+\infty}|\langle\varphi_{n,l,m}|\Phi_e(b,t)\rangle|^2 = \lim_{t\to+\infty}|a_{n,l,m}(b,t)|^2\ . \tag{15}$$

The range of validity of the present single-centered atomic orbital (AO) (coupled-channel) model should be $v_p/Z_p\gg 1$ due to the insufficient treatment of projectile-centered states, which dominate the collision process at low energies.

If the sum in Eq. (13) includes only the initial state φ_i and the corresponding coefficient a_i is set equal to 1, independent of time, the electronic motion is described in a perturbative way. If, furthermore, the last three terms in Eq. (6) are neglected, the treatment would be reduced to the first-order semiclassical approximation (SCA) with straight-line trajectories. This model yields the same cross sections as the first-order plane-wave Born approximation (PWBA).[35,50] The corresponding range of validity is $V_p/Z_p\gg 3$.[43] Since the Bethe theory,[36] which is also a first-order theory, corresponds to the PWBA only in the limit of high projectile velocities, its range of validity is shifted to even higher incident energies.

The accuracy of the present computer code when restricted to perturbation theory (SCA mode) was checked against PWBA (Refs. 37 and 50) and SCA (Refs. 22 and 31) results for ionization and excitation. From the comparison a relative uncertainty of less than 0.1% for probabilities and about 3% for cross sections was inferred for different final states. It is noted that the uncertainty in the cross section calculations is mainly due to the small number of impact parameter steps and continuum energies considered in this work. The numerical transition matrix elements [Eqs. (13')] agree to within 10^{-4} or better with analytical solutions for transitions between the lowest bound states. Finally, the accuracy of the coupled-channel code was checked against results of the well-established two-center code (AO+) by Fritsch.[47,51] When restricted to the same 20 target-centered bound states the results of both codes agree to within two to three digits for excitation probabilities ranging from 10^{-6} to 0.15. With the present code unitarity can be preserved to within about 10^{-7} if the damping factor F in Eq. (12) is set equal to unity.

B. Computation of stopping powers

Each excited state or each continuum state corresponds to a well-defined energy transfer ΔE or $\varepsilon+I_B$ where the initial-state binding energy is denoted I_B. This energy transfer is the so-called Q value of the reaction. An averaged impact-parameter (b) dependent Q value $\bar{Q}$ may be defined as follows:

$$\bar{Q}(b)=n_e\sum_{f=1}^{\infty}P_{i\to f}(b)\Delta E_{i\to f} + n_e\int_0^{\infty}d\varepsilon\frac{dP_{i\to\varepsilon_f}(b,\varepsilon)}{d\varepsilon}(\varepsilon+I_B)\ , \tag{16}$$

where n_e is the number of target electrons in the subshell. Since the projectile mass m_p is changed to m_p^f when electrons are captured from the target, a meaningful definition of the mean projectile energy loss ΔE_p should be normalized to the initial projectile mass. It is noted that this normalization affects only results of two-center theories. In the model described in Sec. II A captured electrons predominantly show up at continuum energies corresponding to the projectile velocity. Thus the projectile mass and the target mass $m_t=m_t^f$ may be considered constant. In this case the mean projectile energy loss reads

$$\overline{\Delta E_p}(b)=E_p^i-\bar{E}_p^f(b)\ . \tag{17}$$

In Eq. (6) the interaction of the electron cloud with the residual target core was neglected. Thus the projectile scattering angle Θ_p is a more accurate quantity than the

recoil energy in this model. Consequently, we search for a connection between the Q value, the projectile scattering angle, and the projectile energy loss. Considering conservation of energy and momentum it follows that

$$[\bar{E}_p^f(b)]^{1/2}=r(b)+[r^2(b)+s(b)]^{1/2}\ , \tag{18}$$

$$r=\frac{m_p(E_p^i)^{1/2}}{m_p+m_t}\cos[\Theta_p(b)]\ , \tag{18a}$$

$$s=\frac{m_t\bar{Q}(b)+E_p^i(m_t-m_p)}{m_p+m_t}\ , \tag{18b}$$

The stopping power per atom S may be computed directly from the impact-parameter integration of the mean projectile energy loss:

$$S=\int_0^\infty db\ b\overline{\Delta E_p}(b)\ . \tag{19}$$

The stopping power and the mean energy transfer may be decomposed in a nuclear contribution, the transfer of kinetic energy to the target nucleus, and in an electronic contribution. The so-called electronic energy loss S_e may be calculated by substituting $\overline{\Delta E_p}$ in Eq. (19) by the Q value. It should be emphasized that the stopping powers given in this work are dominated ($S_e>0.98S$) by the Q value and thus by the electronic energy loss. However, whenever experimental and theoretical stopping powers are compared to each other, in Sec. III, the exact formulas [Eqs. (16)–(19)] are used.

III. RESULTS AND DISCUSSION

Ionization probabilities and cross sections, calculated as described in Sec. II are compared to experimental data. Afterwards, stopping-power results are discussed, first from a theoretical point of view and finally in comparison with experiments. Ionization dominates the stopping power for intermediate to high incident energies. Thus the accuracy of stopping-power calculations may be estimated from the comparison between experimental and theoretical electron spectra.

Figure 2 displays singly differential electron spectra as a function of the electron energy for different incident energies in H^++He collisions. Two basis sets where used for this collision system. One for low incident energies (<40 keV) including about 20 bound target-centered states and one for high incident energies with 6 bound states. It is noted that excitation is important especially at intermediate energies. Bound states have to be included also at low incident energies in order to stimulate electron capture into projectile-centered states at small internuclear distances with a target-centered basis set. Since mean energy transfers are on the order of 20–60 eV, special attention was drawn to achieve reasonable convergence within the partial-wave expansion for the energy regime below 100 eV.

The experimental data include uncertainties of about 20%. The general slopes of the experimental electron spectra are reproduced correctly by the results of the

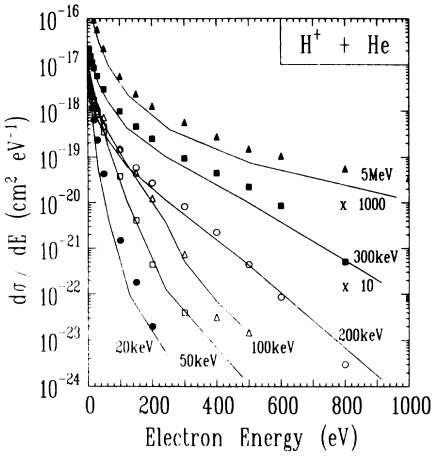

FIG. 2. Singly differential ionization cross sections for 20–5000-keV H^++He collisions. Present theory: solid lines. Experimental data from Ref. 35: triangles, squares, and circles.

coupled-channel calculation. As can be seen from Fig. 2, theoretical predictions agree with experimental data to within $<15\%$ at electron energies below 100 eV. For higher ejection energies and for either low (<30 keV) or high incident energies (>200 keV) the model calculations underestimate the experimental data by about 50%. This is due to the limited number of basis states (90 gerade states for the whole electron spectrum) taken into account. From the data shown in Fig. 2 an uncertainty of about 5% may be estimated for the calculated stopping powers corresponding to the H^+ charge-state fraction, if the population of bound states is calculated exactly with the coupled-channel code. It is conceivable that the uncertainty may be reduced to about 1% when larger basis sets (about 300 states) are used, as done by other authors.[39,40]

The present computer code may be restricted to perturbation theory (SCA mode) by neglecting all couplings, except for those which lead to transitions from the initial state, $1s$ or $1s^2$ in the case of He, to one of the final states. It was verified that the coupled-channel results agree with predictions of the first-order perturbation theory in the case of small perturbation. Small perturbations correspond to either fast projectiles, large impact parameters, or small projectile charges. Thus the advantages of coupled-channel calculations compared to first-order theories should show up especially at intermediate incident energies and for small impact parameters.

Figure 3 shows doubly differential electron spectra as a function of the electron energy for an electron ejection angle of 40° in 100-keV H^++He collisions. The projectile scattering angle of 1° corresponds to an impact parameter of 0.05 a.u., which is small compared to the He $1s^2$ mean orbital radius (0.7 a.u.).[18] The coupled-channel (AO) results are in perfect agreement with the experimental data[18] to within experimental uncertainties. It is noted that neither the exact classical highest-order theory [dynamic screening classical-trajectory Monte Carlo:[32] (dCTMC)] nor the quantum-mechanical first-order theory (SCA) are in agreement with the coincidence data

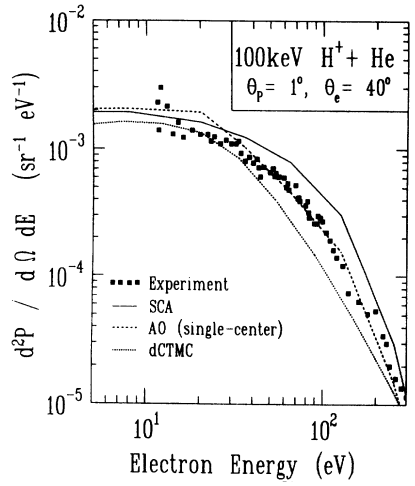

FIG. 3. Doubly differential ionization yields for small impact-parameter 100-keV $H^+ + He$ collisions and an electron ejection angle of 40°. Present theory, full calculation (AO): dashed line; restricted to first-order perturbation theory (SCA): solid line. Classical-trajectory Monte Carlo calculation taken from Ref. 32(b): dotted line. Experimental data taken from Ref. 18: dosed squares.

for intermediate electron energies. Thus it is necessary to use a higher-order theory at intermediate incident energies, even for the lightest projectile ions. Furthermore, it should be kept in mind that predictions of the plane-wave Born approximation for inelastic collisions as well as the Bethe approximation (but only at asymptotically high velocities) are identical to the SCA results. The question remains whether a second-order theory is appropriate or whether a time consuming full coupled-channel calculation is necessary to achieve convergence within the perturbation series.

Figure 4 displays SCA and coupled-channel (AO) results for stopping powers of the H^+ charge-state fraction in an atomic H target calculated with the present code. These values are compared to first-order (O-1) and second-order (O-2) results for an H_2 model molecule described by a set of harmonic oscillators.[20] There is good agreement between both first-order results. It is noted that the molecular binding correction as included in Ref. 20 would reduce the SCA stopping powers by less than 3%. However, there are significant discrepancies between the second-order and the highest-order (AO) results. This is an indication for the importance of higher-order contributions to the stopping power. These higher-order contributions correspond to a Z_p^n behavior (with $n > 3$) of the stopping power. It is thus interesting to investigate the projectile-charge dependence of the stopping power within the AO model, which includes all terms in Z_p.

Figure 5 displays the ratio of stopping powers calculated with the AO model to the corresponding SCA values for protons, antiprotons, α particles, and Li^{3+} ions. SCA, PWBA as well as the Bethe approximation do scale with the squared projectile charge. Hence any deviation of the ratio from unity corresponds to a deviation from the Z_p^2 law. First, it is noted that the antiproton data are not equal to $1\text{-}R(H^+)$, where $R(H^+)$ is the ratio for protons. Also, the proton data below 200 keV correspond to ratios larger than unity, whereas R is smaller than 1 for the heavier positively charged ions. Both facts clearly show that the Barkas term (proportional to Z_p^3) is not sufficient to describe the stopping powers accurately. It is evident that, when there is a high probability for an electron to undergo two-step transitions in a single collision, three-step or multistep processes might be also of importance.

The physical reason for the enhanced proton stopping power compared to the other projectiles is the possibility

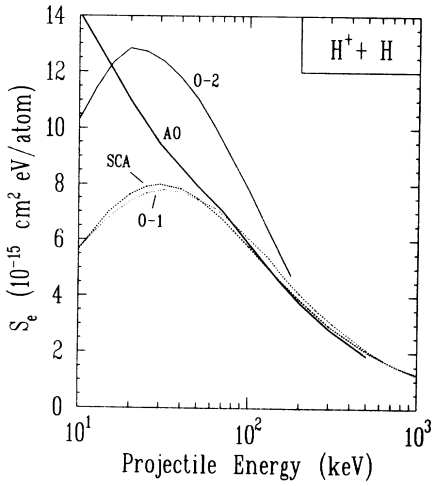

FIG. 4. Theoretical electronic stopping power values for the H^+ charge-state fraction in collisions with hydrogen atoms. Present theory, full calculation (AO): thick solid line, restricted to first-order perturbation theory (SCA): thick dotted line. Results for an H target represented by an harmonic oscillator taken from Ref. 20, first-order perturbation theory (O-1): dotted line; second-order perturbation theory (O-2): solid line.

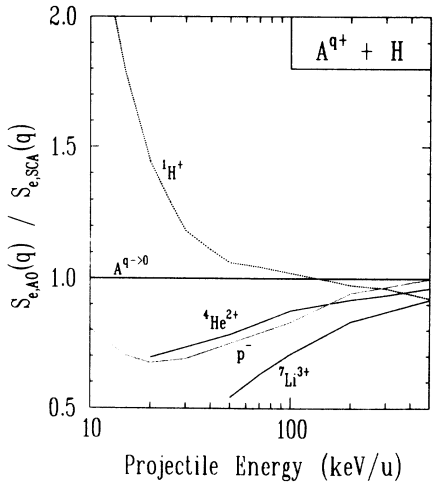

FIG. 5. Ratio of stopping powers, calculated with the present model, to the first-order results computed with an identical set of wave functions, as function of the incident energy for different bare ions penetrating an atomic hydrogen target. Results for projectiles with hypothetical charge states small compared to one fall onto the thick solid line for the ratio of 1.

of resonant electron-capture processes in addition to excitation and ionization of the target atom. In the case of heavier positive ions there is a reduced capture probability since the collision systems are asymmetric with respect to the nuclear charges. The increased binding due to the presence of a positively charged particle leads to a further reduction of the stopping power. In the case of negative projectiles the target atom is polarized so that there is a reduced electron density on the projectile path and thus a reduced stopping power. From the data in Fig. 5, it is possible to conclude that the mean range for antiprotons exceeds the corresponding mean range for protons. This is in accordance with the findings of Barkas and coworkers for π^+ and π^- particles.[10] In order to distinguish the influence of polarization, electron capture, or binding effect on the stopping power, it is interesting to investigate the impact-parameter dependence of the mean energy transfer in $H^+ + H$ collisions.

In Figs. 6 and 7 the mean electronic and nuclear energy transfer in $p^- + H$ and $H^+ + H$ collisions is plotted versus the impact parameter. In Fig. 6 (100-keV $p^- + H$ and $H^+ + H$) there are only minor differences between AO results for the mean energy transfer of proton and antiprotons and the SCA results. Target polarization leads to a slightly enhanced proton electronic stopping power and a reduced antiproton stopping power. However, there are significant deviations for the nuclear energy loss. These deviations do result from the *dynamic* curved projectile trajectories as defined by Eqs. (6) and (6'). The SCA data correspond to scattering of a classical projectile in a *static* screened target potential. The AO results for protons or antiprotons are strongly influenced by polarization effects. In the case of antiprotons the electron density distribution is shifted away from the projectile path. Thus, even at large impact parameters, the projectile interacts with a partially unscreened

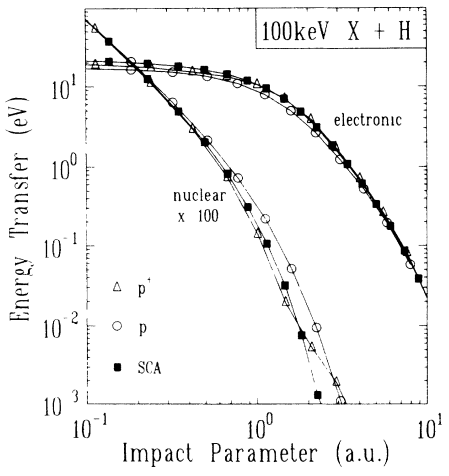

FIG. 6. Theoretical results for the mean nuclear and electronic energy transfer in 100-keV $X^{q+} + H$ collisions as function of the impact parameter. Present theory for protons: triangles; for antiprotons: circles; and restricted to first-order perturbation theory: solid squares.

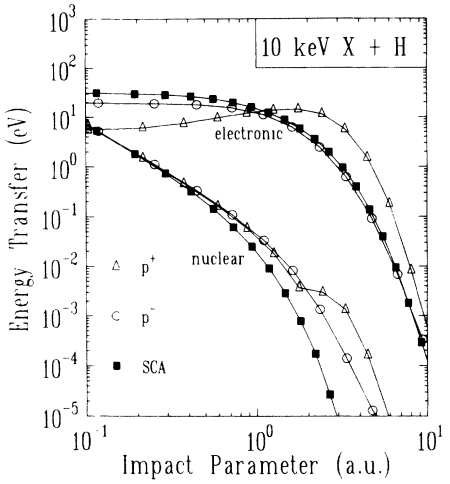

FIG. 7. Theoretical results for the mean nuclear and electronic energy transfer in 10-keV $X^{q+} + H$ collisions as function of the impact parameter. Present theory for protons: triangles; for antiprotons: circles; and restricted to first-order perturbation theory: solid squares.

target system. This leads to an enhanced nuclear stopping compared to the SCA results. In the case of protons at large impact parameters (> 3 a.u.) the electron cloud is attracted by the positively charged particle. Subsequently, there is a negative target net charge and the projectile is deflected *towards* the target nucleus. For small impact parameters the situation on the incoming and outgoing path is similar, but for small internuclear distances both nuclei interact with each other independent of the electronic density distribution. Because the target system is pulled by the projectile at large distances and pushed away at small distances, both forces cancel, partially leading to a reduced nuclear stopping. The broad structure in the nuclear energy-transfer curve for protons at 2 a.u. corresponds to a zero crossing of the mean projectile scattering angle.

The situation in Fig. 7 is similar to the one described above, but the small polarization effect visible for 100-keV projectiles is substituted by the influence of electron capture in 10-keV $H^+ + H$ collisions. As it may be inferred from two-center calculations,[7,32,47] at large impact parameters electron capture dominates the mean electronic energy transfer for protons. This leads to a slightly different impact-parameter dependence of the proton nuclear energy transfer as compared to Fig. 6. The broad structure in the proton nuclear energy transfer is shifted from about 2 a.u. at 100 keV to about 3 a.u. for an incident energy of 10 keV. This is consistent with an enhanced polarization effect which cannot be distinguished from electron capture at low proton velocities. It is interesting to note that the nuclear energy transfer for protons at impact parameters below 2 a.u. is higher than the SCA prediction. Probably this is due to a reduction of the distance of closest approach as a result of the strong polarization on the incoming projectile path. For protons at small impact parameters and at low velocities the mean electronic energy transfer is reduced in compar-

ison with SCA or antiproton data. This is due to the increased binding of the target electron in the projectile Coulomb potential.

Finally, in Figs. 8 and 9 total model stopping-power values are compared to experimental data. It is noted that the experimental data were taken for thick gas targets and correspond to an equilibrated charge-state distribution. The equilibrium fractions for hydrogen beams in H_2 or He targets may be found in the review of Allison.[52] The role of excited projectile states in dense matter is discussed extensively in the literature.[53–58] However, for gas targets it is generally accepted that excited projectile states are of minor importance because, for low collision frequencies, most excited states decay optically to the ground state. Thus the present AO results were weighted with the H^+ charge-state fraction and summed up with the contribution from the reaction $H^0+H^0 \rightarrow H^0+H^+ + e^-$. The latter process involves a neutral collision system and corresponds to a relatively small perturbation. Hence excitation and ionization cross sections for this process were calculated within the PWBA as described by Bates and Griffing.[50]

Figure 8 shows experimental data of different groups[59–63] for $H+H_2$ in comparison with the theoretical results for $H+H$ discussed above. Except for intermediate incident energies, there is agreement between experimental and theoretical data to within 5% or better. At energies around 50 keV the model predictions underestimate the experimental data by 10–15 %. Using PWBA calculations it was checked that the molecular character of the H_2 targets will affect the stopping power values by less than 5% at intermediate energies. Most

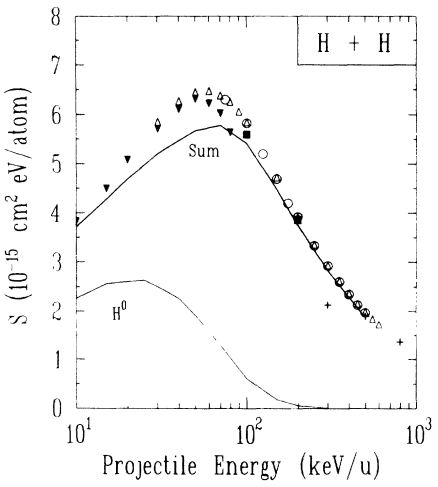

FIG. 8. Equilibrium mean total stopping power per atom for $H+H$ collisions. Exact PWBA results for single excitation and ionization in H^0+H^0 collisions times the corresponding charge-state fraction: thin solid line. Sum of the present coupled-channel results weighted with the H^+ charged-state fraction (taken from Ref. 52) and the H^0 contribution: thick solid line. Experimental data for H projectiles penetrating a thick H_2 target: Ref. 59 (squares), Ref. 60 (circles), Ref. 61 (crosses), Ref. 62 (open triangles), and Ref. 63 (closed triangles).

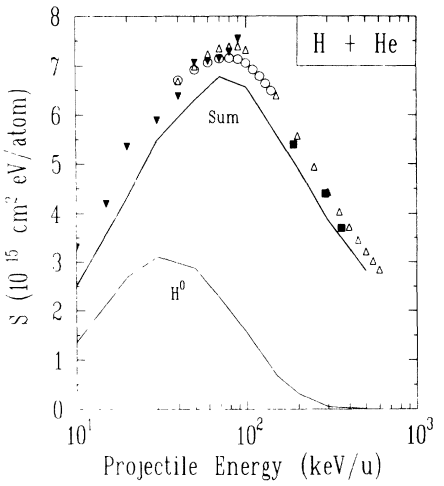

FIG. 9. Equilibrium mean total stopping power per atom for $H+He$ collisions. PWBA results for single excitation and ionization in H^0+He^0 collisions, using hydrogenlike wave functions, times the corresponding charge-state fraction: thin solid line. Sum of the present coupled-channel results weighted with the H^+ charged-state fraction (taken from Ref. 52); and the H^0 contribution: thick solid line. Experimental data for H projectiles penetrating a thick He target: Ref. 62 (open triangles), Ref. 63 (closed triangles), Ref. 65 (squares), and Ref. 66 (circles).

likely, the deviation between experimental and theoretical results corresponds to underestimated ionization cross sections for H^0+H^0 collisions. Electron correlation might lead to simultaneous ionization of both collision partners and may increase ionization cross sections by up to a factor of 2.[64] This could enhance the stopping powers by 10–15 % at the incident energy of 100 keV.

Figure 9 displays experimental data[62,63,65,66] for $H+He$ in comparison with model predictions similar to Fig. 8. The deviations between experimental and theoretical results are about 20% at low energies and less than 10% at intermediate to high incident energies. It is noted that the convergence with respect to the number of basis states seems to be not as good for helium as for hydrogen targets, especially at high continuum energies (corresponding to large momentum transfer collisions). This might explain the uncertainty at high incident energies, where high continuum energies yield a significant contribution to the stopping power. However, below 40 keV the dominant contribution to the total stopping power stems from the neutral hydrogen-beam fraction and is calculated with the PWBA. Because of two reasons the present PWBA calculation for H^0+He is less reliable than for H^0+H^0. First, perturbation theory might break down in the case of projectile ionization by the He target. Second, in the case of He ionization and excitation the target is represented by hydrogenlike wave functions which deviate significantly from more sophisticated He target wave functions.

IV. CONCLUSIONS

An improved stopping-power theory with exact atomic target-centered wave functions for bound states and

damped continuum wave packets is introduced in this work. For the first time a coupled-channel theory is applied to the calculation of stopping powers. Dynamic curved projectile trajectories are introduced, which are sensitive to the time-dependent electron density distribution.

Results from the present theory agree reasonably well with experimental data for ionization in single-collision experiments as well as with stopping powers for protons in thick H and He targets. It is shown that protons suffer an exceptionally high energy loss compared to antiprotons, α particles, and Li^{3+} ions at incident energies below 100 keV/u. This may be viewed as part of a Z_p oscillation of the stopping power, often discussed in the literature. Clearly, a Barkas correction is not able to describe the deviations from first-order perturbation theory found in this work. Furthermore, it is evident that polarization of the electron density distribution leads to drastical changes of the nuclear energy loss, especially at large impact parameters.

It is conceivable that the uncertainties of the stopping-power predictions may be further reduced to about 1% at incident energies above 150 keV/u or below 30 keV/u when larger basis sets are incorporated into the calculation or when two-center or even triple-center theories are used. However, at intermediate energies (30–150 keV/u) there is a 10% contribution to the stopping power, which is consistent with ionization via electron-electron interactions in H^0+H^0 collisions. Thus it appears necessary to include electron correlation in the model to further increase the accuracy at intermediate incident energies. In conclusion, the major problems connected with the slowing down of bare ions in gas targets seem to be solved.

ACKNOWLEDGMENTS

The author would like to thank J. P. Biersack, A. Salin, N. Stolterfoht, I. Kádár, J. F. Reading, J. Eichler, U. Wille, and W. Fritsch for helpful and interesting discussions and B. Skogvall for his help in improving the speed of the computer code.

[1]N. Bohr, Philos. Mag. **25**, 10 (1913).
[2]O. B. Firsov, Zh. Eksp. Teor. Fiz. **9**, 1076 (1959).
[3]H. Bethe, Ann. Phys. (Leipzig) **5**, 325 (1930).
[4]S. K. Allison and S. D. Warshaw, Rev. Mod. Phys. **25**, 779 (1953); S. K. Allison, *ibid.* **30**, 1137 (1958).
[5]H.-D. Betz, Rev. Mod. Phys. **44**, 465 (1972).
[6]J. F. Ziegler, J. P. Biersack, and U. Littmark, *The Stopping and Range of Ions in Solids* (Pergamon, New York, 1985).
[7]G. Schiwietz and W. Fritsch, J. Phys. B **20**, 5463 (1987).
[8]U. Wille and R. Hippler, Phys. Rep. **132**, 129 (1986).
[9]L. G. J. Boesten, T. F. M. Bonsen, and D. Banks, J. Phys. B **8**, 628 (1975).
[10]W. H. Barkas, W. Birnbaum, and F. M. Smith, Phys. Rev. **101**, 778 (1956); W. H. Barkas, J. N. Dyer, and H. H. Heckman, Phys. Rev. Lett. **11**, 138 (1963).
[11]H. H. Andersen, H. Simonsen, and H. Sørensen, Nucl. Phys. **A125**, 171 (1969).
[12]L. H. Andersen, P. Hvelplund, H. Knudsen, S. P. Møller, K. Elsener, K. G. Rensfelt, and E. Uggeerhøj, Phys. Rev. Lett. **57**, 2147 (1986); L. H. Andersen, P. Hvelplund, H. Knudsen, S. P. Møller, A. H. Sørensen, K. Elsener, K. G. Rensfelt, and E. Uggeerhøj, Phys. Rev. A **36**, 3612 (1987).
[13]J. F. Reading and A. L. Ford, Phys. Rev. Lett. **58**, 543 (1987); J. Phys. B **20**, 3747 (1987); R. E. Olson, Phys. Rev. A **36**, 1519 (1987).
[14]A. Jakob, D. Trautmann, F. Rösel, and G. Baur, Nucl. Instrum. Methods **232**, 218 (1984).
[15]J. C. Ashley, R. H. Ritchie, and W. Brandt, Phys. Rev. B **5**, 2393 (1972).
[16]J. D. Jackson and R. L. McCarthy, Phys. Rev. B **6**, 413 (1972).
[17]K. W. Hill and E. Merzbacher, Phys. Rev. A **9**, 156 (1974).
[18]G. Schiwietz, Phys. Rev. A **37**, 370 (1988).
[19]G. Schiwietz, B. Skogvall, N. Stolterfoht, D. Schneider, V. Montemayor, and H. Platten, Nucl. Instrum. Methods B **40/41**, 178 (1989).
[20]H. H. Mikkelsen and P. Sigmund, Phys. Rev. A **40**, 101 (1989).
[21]J. Bang and J. M. Hansteen, K. Dan. Vidensk. Selsk. Mat. Fys. Medd. **31**, 13 (1959).
[22]G. Baur, M. Pauli, and D. Trautmann, Nucl. Phys. **A211**, 333 (1974).
[23]J. H. McGuire and L. Weaver, Phys. Rev. A **16**, 41 (1977).
[24]E. Clementi and C. Roetti, At. Data Nucl. Data Tables **14**, 177 (1974).
[25]N. Stolterfoht, C. C. Havener, R. A. Phaneuf, J. K. Swenson, S. M. Shafroth, and F. W. Mayer, Phys. Rev. Lett. **57**, 74 (1986).
[26]R. Mann and H. Schulte, Z. Phys. D **4**, 343 (1987).
[27]J. A. Tanis, D. Schneider, S. Chantrenne, M. H. Prior, R. Herrmann, R. Hutton, and G. Schiwietz (unpublished).
[28]J. H. McGuire, N. Stolterfoht, and P. R. Simony, Phys. Rev. A **24**, 97 (1981).
[29]L. Kocbach, J. U. Andersen, E. Laegsgaard, and M. Lund, in *Proceedings of the Tenth International Conference on the Physics of Electronic and Atomic Collisions, Paris, 1977,* edited by G. Watel (North-Holland, Amsterdam, 1977), p. 42.
[30]M. Kleber and K. Unterseer, Z. Phys. A **292**, 311 (1979).
[31]F. Rösel, D. Trautmann, and G. Bauer, Nucl. Instrum. Methods **192**, 43 (1982).
[32](a) V. Montemayor and G. Schiwietz, J. Phys. B **22**, 2555 (1989); (b) Phys. Rev. A **40**, 6223 (1989); see also Ref. 7.
[33]R. E. Olson and A. Salop, Phys. Rev. A **16**, 531 (1977).
[34]Dz. Belkic, R. Gayet, and A. Salin, Phys. Rep. **56**, 279 (1979).
[35]S. T. Manson, L. H. Toburen, D. H. Madison, and N. Stolterfoht, Phys. Rev. A **12**, 60 (1975).
[36]M. Inokuti, Rev. Mod. Phys. **43**, 297 (1971).
[37]A. Salin (private communication).
[38]R. D. Cowan, *The Theory of Atomic Structure and Spectra* (University of California Press, London, 1981).
[39]H.-J. Bär and G. Soff, Physica **128C**, 225 (1985).
[40]U. Heinz, W. Greiner, and B. Müller, Phys. Rev. A **23**, 562 (1980).
[41]J. F. Reading, A. L. Ford, G. L. Swafford, and A. Fitchard, Phys. Rev. A **20**, 130 (1979).
[42]N. Stolterfoht, D. Schneider, J. Tanis, H. Altevogt, A. Salin, P. D. Fainstein, R. Rivarola, J. P. Grandin, J. N. Scheurer, D. Bertault, and J. F. Chemin, Europhys. Lett. **4**, 899 (1987).

[43]D. Schneider, D. DeWitt, A. S. Schlachter, R. E. Olson, W. G. Graham, J. R. Mowat, R. D. DuBois, D. H. Loyd, V. Montemayor, and G. Schiwietz, Phys. Rev. A **40**, 2971 (1989).
[44]P. D. Fainstein and R. Rivarola, J. Phys. B **20**, 1285 (1987).
[45]T. G. Winter, Phys. Rev. A **25**, 697 (1982).
[46]J. F. Reading, A. L. Ford, and R. L. Becker, J. Phys. B **14**, 1995 (1981).
[47]W. Fritsch and C. D. Lin, J. Phys. B **15**, 1255 (1982); Phys. Rev. A **27**, 3361 (1983).
[48]D. F. Gallaher and L. Wilets, Phys. Rev. **169**, 139 (1968).
[49]T. Winter and C. D. Lin, Phys. Rev. A **29**, 3071 (1984).
[50]D. R. Bates and G. Griffing, Proc. Phys. Soc. A **66**, 961 (1953).
[51]W. Fritsch (private communication).
[52]S. K. Allison, Rev. Mod. Phys. **30**, 1137 (1958).
[53]N. Bohr and J. Lindhard, Dan. Mat. Fys. Medd. **28**, (1954).
[54]H.-D. Betz and L. Grodzins, Phys. Rev. Lett. **25**, 211 (1970); see also Ref. 5.
[55]R. A. Baragiola, P. Ziem, and N. Stolterfoht, J. Phys. B **9**, L447 (1976).
[56]J. D. Garcia, R. J. Fortner, H. C. Werner, D. Schneider, N. Stolterfoht, and D. Ridder, Phys. Rev. A **22**, 1884 (1980).
[57]G. Schiwietz, Radiat. Eff. Defects Solids **112**, 195 (1990).
[58]J. Rozet, A. Chetioui, P. Piquemal, D. Vernhet, K. Wohrer, and C. Stephan, J. Phys. B **22**, 33 (1989).
[59]E. Bonderup and P. Hvelplund, Phys. Rev. A **4**, 562 (1971).
[60]S. D. Warshaw, Phys. Rev. **76**, 1759 (1949).
[61]R. A. Langley, Phys. Rev. B **12**, 3575 (1975).
[62]H. K. Reynolds, D. N. F. Dunbar, W. A. Wenzel, and W. Whaling, Phys. Rev. **92**, 742 (1953).
[63]J. A. Phillips, Phys. Rev. **90**, 532 (1953) (*d* and *t* projectiles were used for incident energies below 40 keV).
[64]R. Shingal, B. H. Bransden, and D. R. Flower, J. Phys. B **22**, 855 (1989).
[65]P. K. Weyl, Phys. Rev. **91**, 289 (1953).
[66]J. T. Park and E. J. Zimmermann, Phys. Rev. **131**, 1611 (1963).